Novel Fe/Ca oxide co- embedded coconut shell biochar for phosphorus recovery from agricultural return flows

Anqi Hu [a,c†], Yongcan Jiang [a,b†] *, Jiaqi An [c], Xiaodian Huang [a], Abdelbaky Hossam Elgarhy [c,d], Huafen Cao [c], Guanglong Liu [c] *

Affiliation

[a] PowerChina Huadong Engineering Corporation Ltd., Hangzhou 311122, Zhejiang Province, China;

[b] Institute of Soil and Water Resources and Environmental Science, College of Environmental and Resource Sciences, Zhejiang University, Hangzhou 310058, Zhejiang Province, China;

[c] State Environmental Protection Key Laboratory of Soil Health and Green Remediation, College of Resources and Environment, Huazhong Agricultural University, Wuhan 430070, China;

[d] Central Laboratory for Environmental Quality Monitoring (CLEQM), National Water Research Center (NWRC), Qalyobia, 13621, Egypt.

*Corresponding author:

Prof. Guanglong Liu. E-mail: liugl@mail.hzau.edu.cn

† Contributed equally to this work.

Text S1

The phosphate removal efficiency (%) and adsorption capacity (Q_e) of the modified biochar were calculated using Eq. (1) and Eq. (2).

$$Removal\ efficiency = \left(\frac{C_0 - C_e}{C_0}\right) \times 100\% \quad (1)$$

$$Q_e = \frac{C_0 - C_e}{m} V \quad (2)$$

where C_0 and C_e (mg/L) represent the initial and final phosphate concentrations, respectively; V (L) stands for the volume of the solution; m (g) denotes the mass of the biochar.

Effect of dosage and pH on phosphorus adsorption

Adsorption experiments were conducted to compare the phosphorus adsorption at various dosages to determine the optimum dosage. The dosages were set as 0.1, 0.5, 1, 1.5, 2, 4, 6, and 8 g/L, and the above dosages of FCBC and BC were mixed with 250 mL of KH_2PO_4 solution (50 mg/L, pH = 8), respectively. To investigate how pH impacts the adsorption of phosphorus by FCBC, 0.5 g of FCBC was mixed with 250 mL of KH_2PO_4 solution (50 mg/L). The solution's pH was set to 2, 4, 6, 8, 10, and 12, respectively. The content of remaining phosphorus and pH in the solution were measured by oscillating at 20°C for 12 h.

Adsorption isotherm and kinetics experiments

The adsorption isotherms were investigated by combining 0.5 g of FCBC with 250 mL of KH_2PO_4 solution at different concentrations (5 - 500 mg/L). The experimental data was simulated using two models: the Langmuir model (Eq. 3) and the Freundlich model (Eq. 4).

$$Q_e = \frac{K_L Q_m C_e}{1 + K_L C_e} \tag{3}$$

$$Q_e = K_F C_e^{\frac{1}{n}} \tag{4}$$

where Q_e (mg/g) stands for the quantity of phosphate adsorbed at the equilibrium concentration of the phosphate solution (C_e, mg/L); K_L (L/mg) and K_F ($mg^{1-1/n} \cdot g^{-1} \cdot L^{1/n}$) represent the Langmuir and Freundlich constants, respectively; Q_m (mg/g) denotes the maximum adsorption capacity; 1/n is an empirical constant for the Freundlich model.

The adsorption kinetics at different contact times from 0 to 24 h were investigated by combining 0.5 g of FCBC and 250 mL of KH_2PO_4 solution (50 mg/L, pH = 8). The adsorption mechanism of FCBC on phosphate was determined using the pseudo-first-order (Eq. 5), pseudo-second-order (Eq. 6), and intra-particle diffusion models (Eq. 7).[1]

$$Q_t = Q_e\left(1 - \exp\left(-k_1 t\right)\right) \tag{5}$$

$$Q_t = \frac{k_2 Q_e^2 t}{1 + k_2 Q_e t} \tag{6}$$

$$Q_t = k_i t^{0.5} + C \tag{7}$$

where k_1 and k_2 represent the rate constants for the pseudo-first-order and pseudo-second-order models, respectively; k_i and C are the intra-particle diffusion rate constant and intercept, respectively; Q_t (mg/g) denotes the quantity of phosphate adsorbed at time t, and Q_e (mg/g) is the quantity of phosphate adsorbed at equilibrium.

Effect of coexisting anions

To investigate the impact of common coexisting anions on phosphorus elimination by biochar, varying quantities of Na_2CO_3, $NaNO_3$, Na_2SO_4, $NaHCO_3$, NaF, and NaCl were introduced into a 250 mL KH_2PO_4 solution (50 mg/L). This resulted in coexisting anion concentrations of 100, 500, and 1000 mg/L in the prepared solution. Then, 0.5 g of FCBC was weighed and mixed with a KH_2PO_4 solution containing coexisting anions.

Adsorption of phosphorus from natural waters

To further examine the adsorption effect of FCBC and BC on phosphorus in natural water bodies, samples of farmland tailwater, ditch water, and pond water were collected from agricultural surface sources in the test field area of Keyuan Road, Wuhan City, Hubei Province, China, on October 11, 2023. The reactor was loaded with 0.5 g of FCBC and BC, and then 250 mL of farmland tailwater, ditch water, and pond water were added respectively.

Table S1 Surface area and pore structure of BC and FCBC

	S_{BET} (m^2/g)	Pore volume (cm^3/g)	Pore size (nm)
BC	291.2934	0.218585	4.2745
FCBC	441.5189	0.263961	3.3788

Table S2 Parameters for adsorption kinetics of P on FCBC

Models	Parameter 1	Parameter 2	R^2
Pseudo-first-order	k_1=0.0049	Q_e=18.1213 mg/L	R^2=0.9844
Pseudo-second-order	k_2=0.0002	Q_e=22.2797 mg/L	R^2=0.9939
	k_{i1}=0.8783	C_1=-1.0271	R^2=0.9961
Intraparticle diffusion	k_{i2}=0.6253	C_2=2.4845	R^2=0.9921
	k_{i3}=0.0701	C_3=16.4141	R^2=0.9911

Table S3 Parameters for adsorption isotherm of P on FCBC

Models	Parameter 1	Parameter 2	R^2
Langmuir	K_L=0.01623 L/mg	Q_m=53.3131 mg/g	R^2=0.9982
Freundlich	K_F=4.1684 $mg^{1-1/n}\cdot g^{-1}\cdot L^{1/n}$	1/n=0.4168	R^2=0.9631

Table S4 Comparison of the maximum adsorption capacity of different biochar adsorbents for P

Adsorpant	Isotherm	Kinetics	Q_{max} (mg/g)	References
MgO-modified biochar	F	S	18.98	[2]
Palm waste biochar	L	S	26.90	[3]
Lime sludge modified biochar	R-P	S	15	[4]
Hydrocotyle vulgaris derived novel biochar beads	L	S	20.32	[5]
Fe/Mg-Biochar Nanocomposites	L-F	S	6.95	[6]
Lanthanum-ammonia-modified hydrothermal biochar	L	S	43.1	[7]
ZrO_2 nanoparticles embedded in biochar modified with layered double oxides nanosheets	L	S	20.36	[8]
FCBC	L	S	53.31	This study

F, L, R-P, and S represent Freundlich, Langmuir, Redlich-Peterson, and Pseudo-second-order, respectively.

Table S5 Physical and chemical properties of water samples

Parameters	Samples		
	Ponds	Farmlands	Ditches
pH	8.14±0.064	8.79±0.089	8.02±0.042
DOC (mg/L)	10.3±0.505	11.5±0.156	15.8±0.459
TP (mg/L)	0.34±0.004	0.53±0.005	0.11±0.002
DOP (mg/L)	0.21±0.002	0.37±0.003	0.084±0.001
TN (mg/L)	0.92±0.014	1.13±0.014	0.89±0.014
NO_3^--N (mg/L)	0.150±0.001	0.140±0.001	0.525±0.002
NO_2^--N (mg/L)	0.009±0.002	0.010±0.001	0.072±0.002

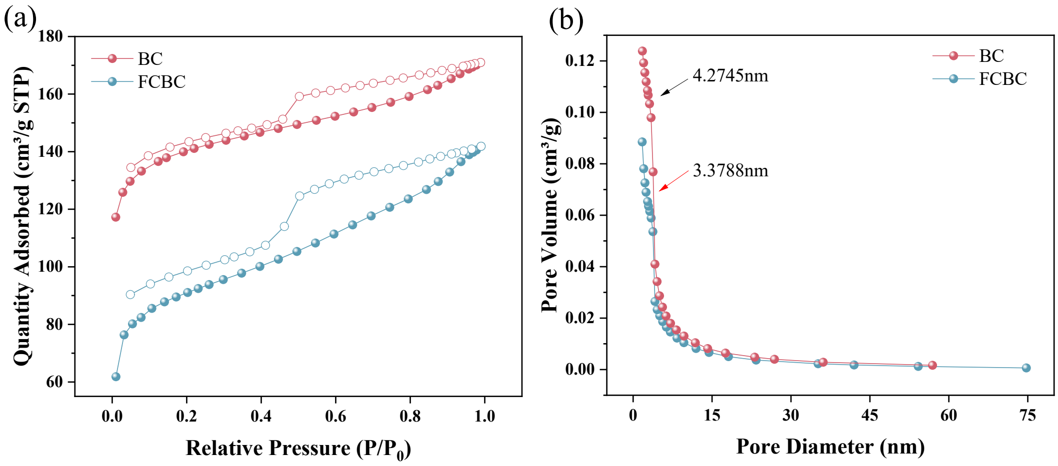

Fig. S1 N_2 adsorption-desorption isotherms (a) and pore size distribution (b) of BC and FCBC

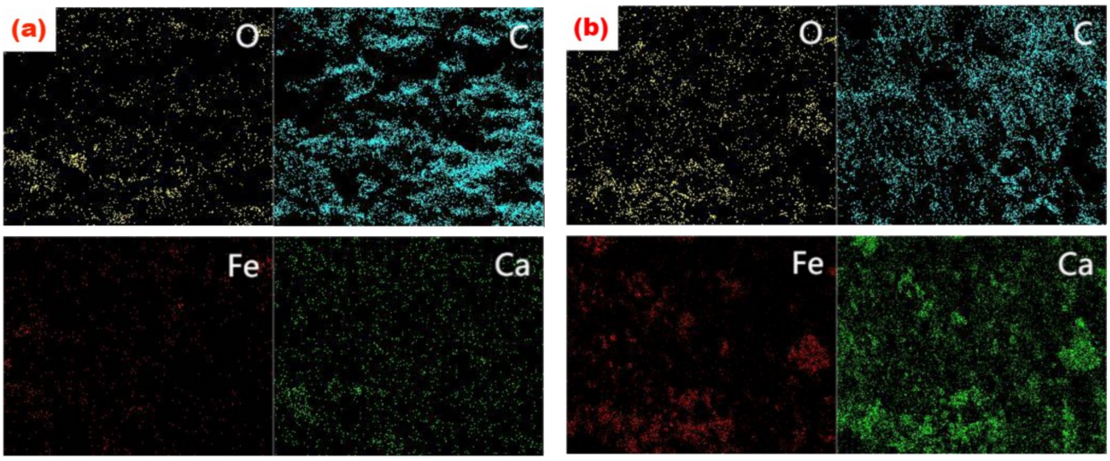

Fig. S2 Element mapping of BC(a) and FCBC(b)

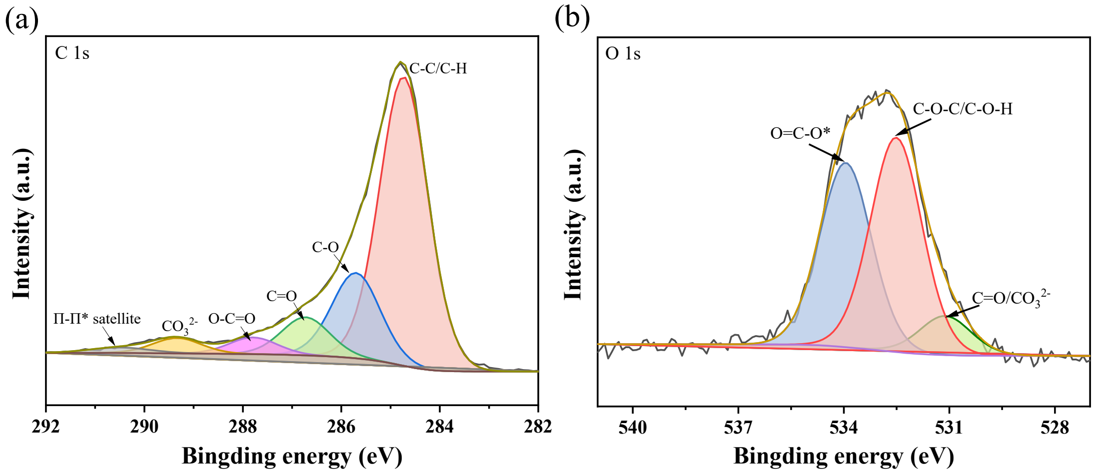

Fig. S3 C 1s (a) and O 1s (b) XPS spectra of BC

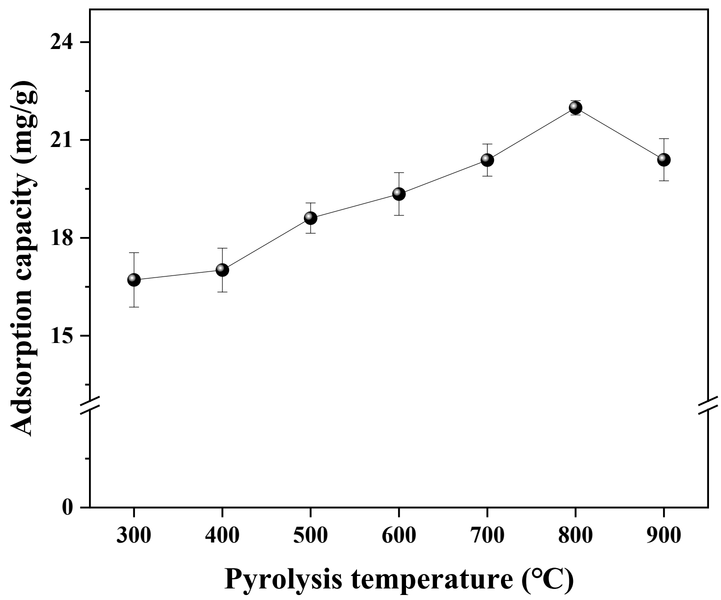

Fig. S4 Phosphorus adsorption capacity of FCBC at different pyrolysis temperatures

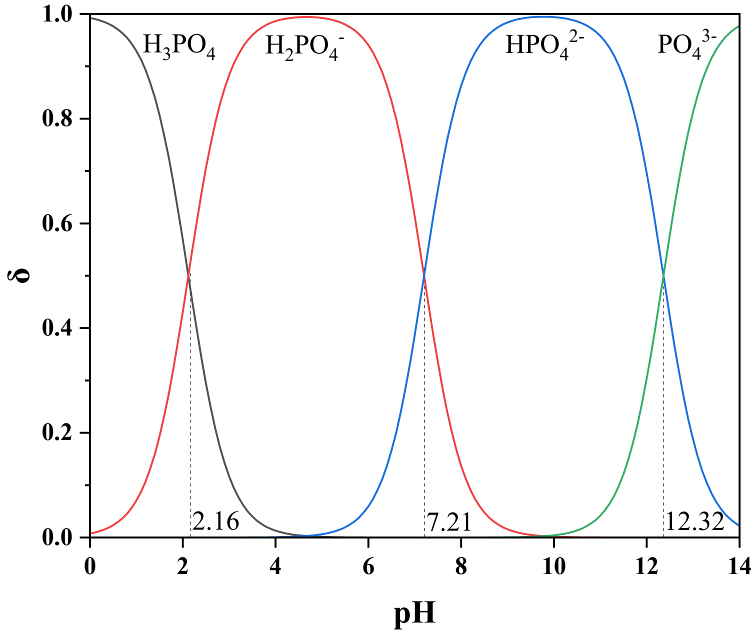

Fig. S5 The abundance ratio of phosphates in solutions of varying pH [9]

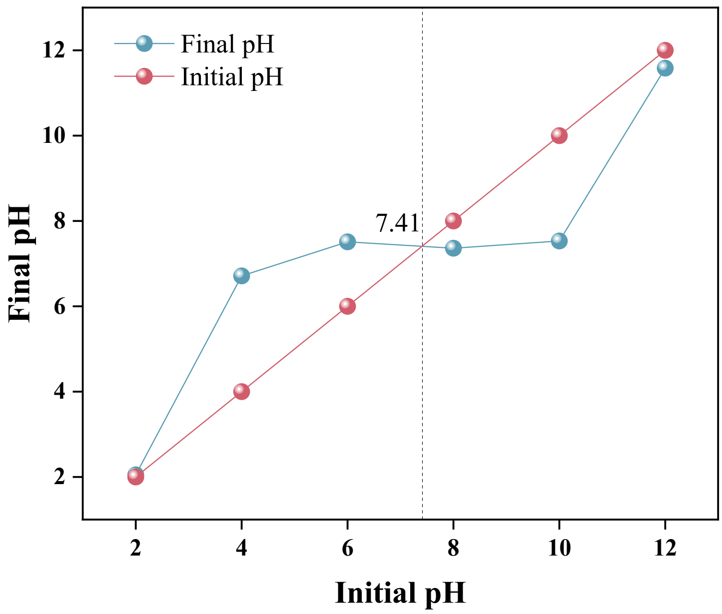

Fig. S6 Determination of the point of zero charge of FCBC

References

1 K.W. Jung, T.U. Jeong, H.J. Kang and K.H. Ahn, Characteristics of biochar derived from marine macroalgae and fabrication of granular biochar by entrapment in calcium-alginate beads for phosphate removal from aqueous solution, *Bioresour. Technol.*, 2016, **211**, 108-116, https://doi.org/10.1016/j.biortech.2016.03.066.

2 L. Wu, C. Wei, S. Zhang, Y. Wang, Y. Kuzyakov and X. Ding, MgO-modified biochar increases phosphate retention and rice yields in saline-alkaline soil, *J. Cleaner Prod.*, 2019, **235**, 901-909, https://doi.org/10.1016/j.jclepro.2019.07.043.

3 Y.H. Fseha, B. Sizirici and I. Yildiz, The potential of date palm waste biochar for single and simultaneous removal of ammonium and phosphate from aqueous solutions, *J. Environ. Chem. Eng.*, 2021, **9**, https://doi.org/10.1016/j.jece.2021.106598.

4 S. Yang, S. Katuwal, W. Zheng, B. Sharma and R. Cooke, Capture and recover dissolved phosphorous from aqueous solutions by a designer biochar: Mechanism and performance insights, *Chemosphere*, 2021, **274**, 129717, https://doi.org/10.1016/j.chemosphere.2021.129717.

5 X. Fu, P. Wang, J. Wu, P. Zheng, T. Wang, X. Li and M. Ren, Hydrocotyle vulgaris derived novel biochar beads for phosphorus removal: static and dynamic adsorption assessment, *J. Environ. Chem. Eng.*, 2022, **10**, https://doi.org/10.1016/j.jece.2022.108177.

6 X. Tao, T. Huang and B. Lv, Synthesis of Fe/Mg-Biochar Nanocomposites for Phosphate Removal, *Materials (Basel)*, 2020, **13**, https://doi.org/10.3390/ma13040816.

7 Z. Shang, Y. Wang, S. Wang, F. Jin and Z. Hu, Enhanced phosphorus removal of constructed wetland modified with novel Lanthanum-ammonia-modified hydrothermal biochar: Performance and mechanism, *Chem. Eng. J.*, 2022, **449**, https://doi.org/10.1016/j.cej.2022.137818.

8 X. Song, X. Chen, W. Chen and T. Ao, ZrO_2 nanoparticles embedded in biochar modified with layered double oxides nanosheets for phosphorus removal by capacitive deionization, *Sep. Purif. Technol.*, 2024, **328**, https://doi.org/10.1016/j.seppur.2023.125117.

9 Q. Yin, H. Ren, R. Wang and Z. Zhao, Evaluation of nitrate and phosphate adsorption on Al-modified biochar: Influence of Al content, *Sci. Total Environ.,* 2018, **631-632**, 895-903, https://doi.org/10.1016/j.scitotenv.2018.03.091.